Radiochim. Acta **100**, 569–578 (2012) / **DOI** 10.1524/ract.2012.1963

The impact of the properties of the heaviest elements on the chemical and physical sciences[#]

By J. V. Kratz*

Institut für Kernchemie, Universität Mainz, 55099 Mainz, Germany

(Received April 2, 2012; accepted in revised form April 24, 2012)
(Published online July 30, 2012)

Transuranium elements / Periodic Table, Atomic structure / Relativistic effects / Nuclear structure / Nuclear shell effects / Fission isomers / Neutron-shell closures in the transactinides / Search for the next spherical proton shell

Summary. The unique role of the heaviest elements in chemical and physical sciences is discussed. With the actinide series ($Z = 90$–103) and the superactinide series ($Z = 122$–155), the heaviest elements have significantly shaped the architecture of the Periodic Table of the elements. Relativistic effects in the electron shells of the heaviest elements change the chemical properties in a given group in a non-linear fashion. Relativistically stabilized sub-shell closures give rise to a new category of elements in the Periodic Table: volatile metals. The prototype for this property is element 114 which, due to the relativistic stabilization of its $7s^2\,7p_{1/2}^2$ electron configuration, is volatile in its elementary state, but, in contrast to a noble gas, exhibits a marked metal-metal interaction with a gold surface at room temperature. Nuclear shell effects dominate the physical properties of the transuranium elements. These give rise to superdeformed shape isomers (fission isomers) in the actinides (U–Bk). Superheavy elements ($Z \geq 104$) owe their existence solely to nuclear shell effects at $N = 152$, 162, and 184. At this time, a building lot is the location of the next spherical proton shell closure as there is evidence that the center of the "island of stability" is not at $Z = 114$. This needs urgently further theoretical and experimental efforts. The cross sections for the syntheses of elements 119 and 120 will give us important information on the "upper end of the Periodic Table of the elements".

1. Introduction

With the TAN'11 being organized in the International Year of Chemistry 2011 proclaimed by the United Nations Educational, Scientific and Cultural Organization, UNESCO, and the International Union of Pure and Applied Chemistry, IUPAC, it was felt to be appropriate to analyse what has been the impact of the synthesis and investigation of the heaviest elements on the chemical science and on our understanding of nuclear stability. Firstly, it is noteworthy that the discovery of 26 transuranium elements has considerably enlarged the Periodic Table of the elements so that almost a quarter of the elements known today are man-made and do not exist in nature. The impact of the properties of these elements on chemical science is reflected in the architecture of the Periodic Table and in the relativistic effects in the electron shells which become a dominant feature for the chemical properties of the heaviest elements. The impact of the heaviest elements on the physical science is the vanishing stability of their nuclei due to the macroscopic liquid drop model, but, on the other hand, their stabilisation by nuclear shell effects. Superheavy elements, as a definition, owe their stability solely to nuclear shell effects. Deformed shell closures at $N = 152$ and 162 are by now firmly established. In this article, the question is asked where the next spherical proton shell is located and an alternative location to the long predicted $Z = 114$ as derived from the periodicities in nuclear properties predicted by the Interacting Boson Approximation is discussed along with possible synthetic routes to search for this new location.

2. Periodic Table of the elements

The Periodic Table was invented in 1869 by Dmitri Mendeleev [1, 3] and independently by Lothar Meyer [2] in order to arrange the elements according to their chemical properties and according to their atomic number. In the Periodic Table of 1871 by Mendeleev, interestingly, the positions of the at that time unknown elements Sc = 44, Ga = 68, Ge 72, and Tc = 100 have been reserved for these elements, demonstrating the predictive power of this arrangement of the elements. The pre-World War II Periodic Table containing 18 groups including one for the noble gases and a lanthanide group, predicted erroneous positions for the transactinium elements. The Periodic Table published in 1945 by G.T. Seaborg [4, 5] showed his placement of the heaviest elements as an actinide ($5f$) series in analogy to the lanthanide ($4f$) series. This had emerged from the successful syntheses of ^{242}Cm in the ^{239}Pu(α,n) reaction in 1944 at the Berkeley 60-inch cyclotron

*E-mail: jvkratz@uni-mainz.de.
The author is a member of the Editorial Board of this journal. Editor.
[#] Based on the opening lecture presented at the 4th International Conference on the Chemistry and Physics of the Transactinide Elements, TAN '11, 5 September 2011, Sochi, Russia.

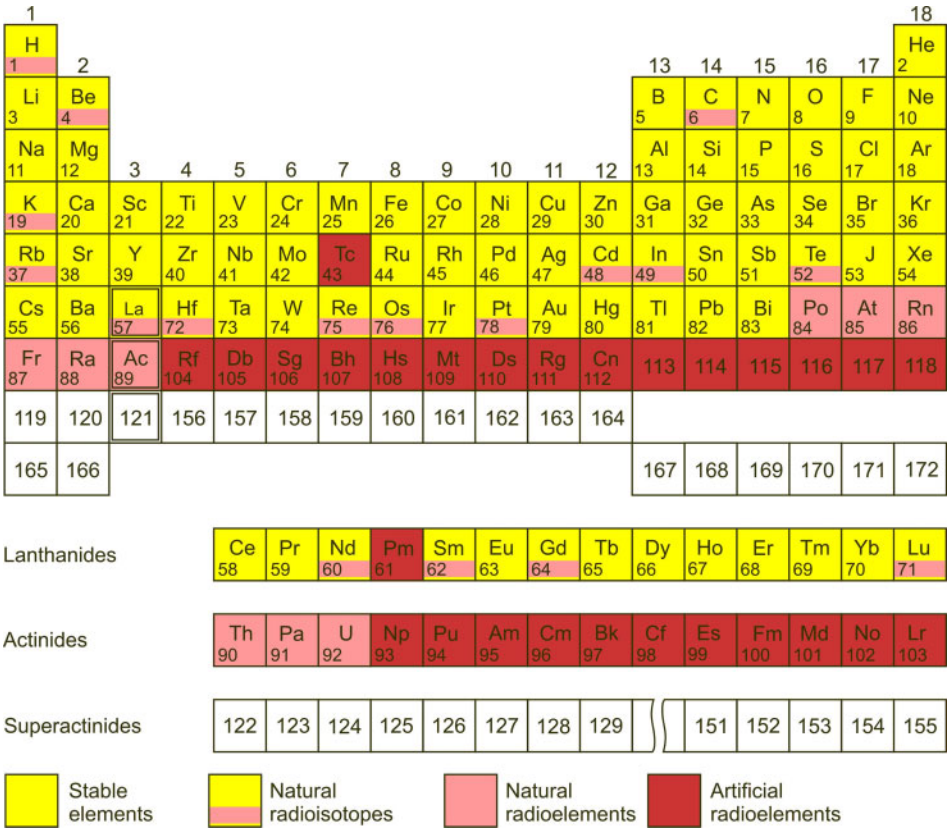

Fig. 1. Present Periodic Table showing elements up to the critical Z_{cr} which is close to $Z = 172$ including an actinide series and a superactinide series.

and of ^{241,242}Am in the Hanford and Clinton piles in the reaction sequence $^{239}\mathrm{Pu}(n,\gamma)^{240}\mathrm{Pu}(n,\gamma)^{241}\mathrm{Pu}\xrightarrow{\beta^-}{}^{241}\mathrm{Am}$; $^{141}\mathrm{Am}(n,\gamma)^{242}\mathrm{Am}\xrightarrow{\beta^-}{}^{242}\mathrm{Cm}$ in 1945, and from the chemical observation that the newly produced activity "is carried by rare earth fluorides and it has not yet been possible to oxidize it to a state or states where its fluoride is soluble." The non-lanthanide like behaviour of the earlier $5f$ elements Th through Pu due to a relativistic delocalization of the $5f$ electrons will be discussed in Sect. 3. Fig. 1 shows a modern Periodic Table based on relativistic atomic calculations by Fricke, Greiner and Waber [6] containing a superactinide series in which $8p_{1/2}$, $6f$, and $5g$ electron orbitals are filled between $Z = 122$ and 155. After the $7d^{10}$ electron configuration in element 164, the $9s$ electrons are filled in elements 165 and 166, the $9p_{1/2}$electrons in elements 167 and 168 and, according to Fricke and Waber [7], the $8p_{3/2}$electrons in elements 169 through 172.

3. Relativistic effects in the chemistry of the transuranium elements

The relativistic mass increase of a particle with velocity υ is

$$m = m_0\left[1-(\upsilon/c)^2\right]^{-1/2}, \tag{1}$$

where m_0 is the mass at zero velocity (rest mass) and c is the speed of light. The Bohr model for a hydrogen-like species gives the following expressions for the velocity, energy, and orbital radius of an electron

$$\upsilon = \left(2\pi e^2/nh\right)Z, \tag{2}$$

$$E = -\left(2\pi^2 e^4/n^2h^2\right)mZ^2, \tag{3}$$

and

$$r = Ze^2/m\upsilon^2, \tag{4}$$

where n is the principal quantum number, e is the elementary charge, and h is Planck's constant. With increasing Z, the ratio m/m_0 increases. For hydrogen, it is 1.000027, and from the 6$^{\text{th}}$ row on, this ratio exceeds 10% so that relativistic effects can no longer be neglected. For element 114, m/m_0 is 1.79, and for element 118, it is 1.95. The energetic stabilization (Eq. 3) and contraction (Eq. 4) of the hydrogen-like s and $p_{1/2}$ orbitals is a direct relativistic effect. This effect was found to be also large for the valence region due to the direct action of the relativistic perturbation operator on the inner part of the valence density [8]. As an example, the $7s$ atomic orbital (AO) of element 112, Cn, is by 10 eV relativistically stabilized and 25% contracted [9].

The indirect relativistic effect causes an expansion and energetic destabilization of the $p_{3/2}$, d, f, and g orbitals, see the behaviour of the d orbitals in Fig. 2, due to increased screening of the nuclear charge by the relativistically contracted s and $p_{1/2}$ AOs. The third important relativistic effect comes from the spin-orbit splitting of the AOs with $l > 0$. All three effects scale approximately with Z^2 for the valence shells in a given group in the Periodic Table. Fig. 3 (left) represents the radial distribution of the valence ns orbitals of Nb, Ta, and Db for electronic configurations d^4s, d^3s^2, and d^3s^2, respectively, according to relativistic Dirac-Slater (DS) and non-relativistic (Hartree–Fock Slater) atomic and molecular calculations [10]. The relativistic contraction of the main maximum are 3%, 9.1%, and 20.5%, respectively. The energetic consequences are shown in Fig. 3 (right). The relativistic stabilization of the ns and destabilization of the (n –

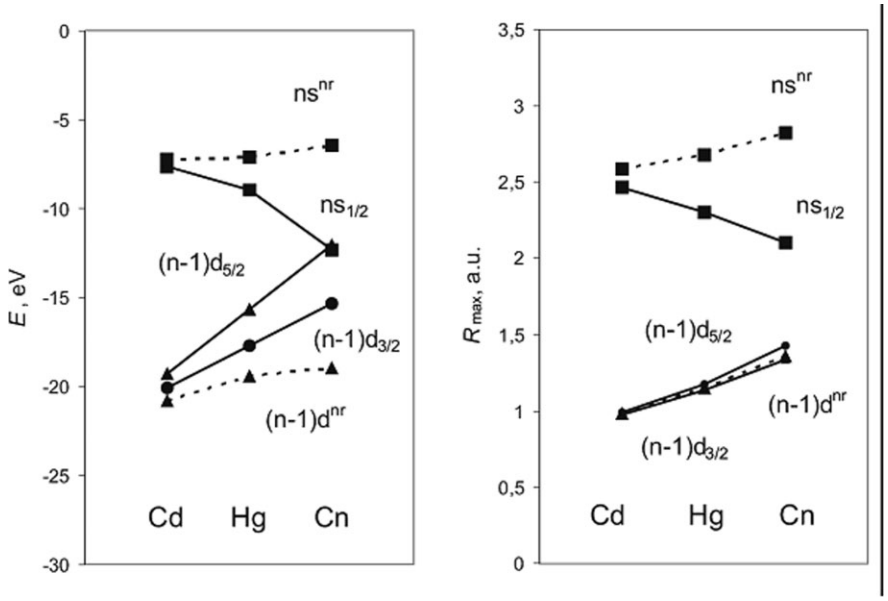

Fig. 2. Relativistic (solid line) and non-relativistic (dashed line) energies and R_{max} of the valence *ns* and $(n-1)d$ AOs of the group-12 elements. The data are from [9]. (Reproduced with the permission of Oldenbourg Wissenschaftsverlag München (Pershina, 2011)).

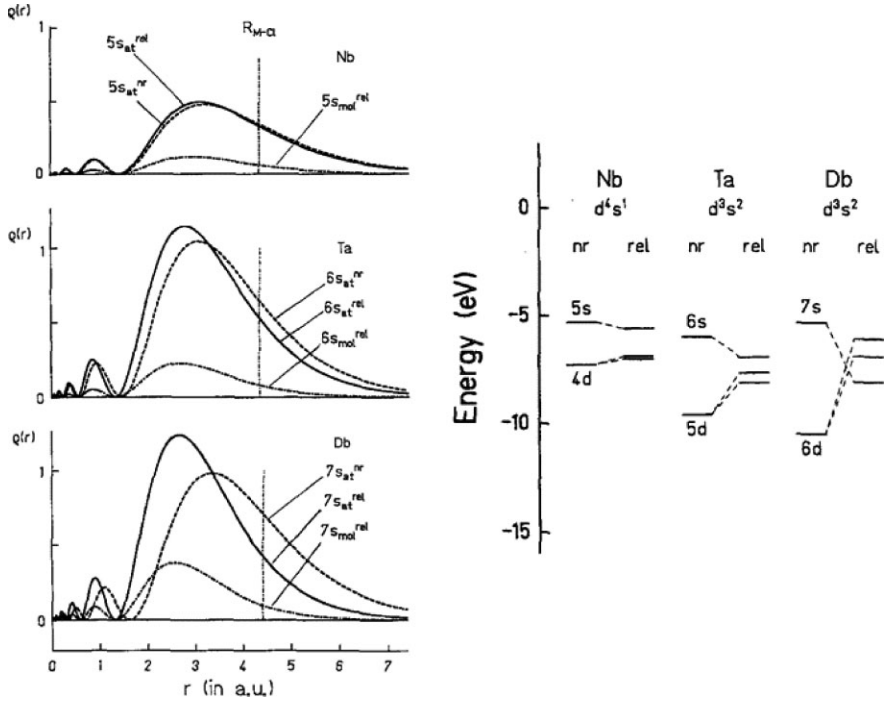

Fig. 3. Left: Radial distribution of the *ns* electrons in Nb, Ta, and Db as a result of the atomic (at) DS relativistic (solid line) and non-relativistic (dashed line) calculations. The dash-dotted lines (mol) are from relativistic calculations of MCl_5. The vertical lines give the bond distance. Right: Binding energies of Nb, Ta, and Db as a result of DF relativistic and HF non-relativistic calculations (Ref. [9]). (Reproduced from Pershina and Fricke (1993). Copyright 1993 American Institute of Physics).

$1)d$ electron energies is demonstrated showing the binding energies in the non-relativistic and relativistic approximations. The spin-orbit splitting of the $(n-1)d$ orbitals increases for Nb, Ta, and Db from 0.14 to 0.48 and to 0.80 eV. The first electron to be ionized in Db is a $6d_{5/2}$ electron and not the 7*s* electron.

Beyond the classical closed-shell configured $6d^{10}\,7s^2$ in element 112, the very large spin-orbit splitting in $7p$ AOs and the strong relativistic stabilization of the $7p_{1/2}$ AOs result in a quasi-closed shell configuration $7s^2\,7p_{1/2}^2$ in element 114. This, together with the relativistic stabilization of the 7*s* AOs renders both elements 112 and 114 to be more inert than their lighter homologs. According to early atomic calculations by Pitzer [11], the promotion energy to the valence state electron configuration $s_{1/2}^2 \rightarrow sp$ in element 112 and $p_{1/2}^2 \rightarrow p^2$ in element 114 will not be compensated by the energy gain of the chemical bond formation. He concluded both elements 112 and 114, Cn and E114, to be very inert, like noble gases, or volatile liquids bound by dispersion forces only. More recent molecular, cluster, and solid-state relativistic calculations on these elements suggest that Cn and E114 are more inert than the lighter homologs in the groups 12 and 14, but still reveal a metallic character [12, 13], *e.g.*, upon M−M′ interactions (M = Cn or E114, M′ = metal, *e.g.* Au). In contrast to Pitzer's conclusion, E114 is expected to provide both $7p_{1/2}$ and $7p_{3/2}$ AOs for metal-metal interactions. Therefore a purely *van der Waals* type interaction typical for a noble gas is no longer anticipated for either element upon adsorption on metal surfaces. The recently measured adsorption enthalpy of Cn on Au ($-\Delta H_{ads}^{Au} = 52^{+4}_{-3}$ kJ mol^{-1}) points at the formation of a weak metal-metal bond [14, 15] with Au. This

is in agreement with recent theoretical calculations [12, 13]. Results of first gas-chemical studies of E114 [16] do not allow for a clear discrimination between a metal- or noble-gas like behaviour. A Monte-Carlo simulation of the adsorption behaviour based on three observed E114 atoms resulted in a value of $-\Delta H_{\mathrm{ads}}^{\mathrm{Au}} = 34^{+54}_{-11}\,\mathrm{kJ\,mol^{-1}}$ at the 95% confidence level. The rather low most probable value was interpreted by the authors as evidence for the formation of a weak physisorption bond [16] between E114 and a gold surface. Unfortunately, the large uncertainty of the reported value covers almost the entire range from a typical metallic behaviour to a noble-gas like behaviour.

The work reported by Yakushev *et al.* [17] made use of a combination of a recoil separator to isolate E114 and a gaschromatography detector system providing significantly improved background conditions compared to previous studies [16] performed without preseparation. In this experiment, E114 in its elemental state was transported with a carrier gas through two COMPACT detector arrays each consisting of 32 pairs (gap: 0.6 mm) of PIN diodes covered by a ≈ 50 nm thick gold layer. COMPACT I was run isothermally at room temperature, COMPACT II with a negative temperature gradient. Two decay chains from ^{288,289}114 were detected. Both E114 decays were detected in COMPACT I at room temperature. The last two members of the chain starting from ^{285}Cn decayed in COMPACT II at $-32\,^{\circ}$C, consistent with the adsorption enthalpy of [14, 15]. The deposition pattern of E114, using Monte Carlo modelling, is defining $-\Delta H_{\mathrm{ads}}^{\mathrm{Au}} > 48\,\mathrm{kJ\,mol^{-1}}$ as a lower limit for the adsorption enthalpy of E114 on gold at 95% c.l. This value reveals a metallic character upon adsorption on gold due to the formation of a metal-metal bond which is at least as strong as that of Cn. This is in agreement with theory [12, 13]. To conclude, this experiment establishes that element 114 is a volatile metal.

Thus, relativistic effects have created a new category of elements in the Periodic Table: Cn and E114 are volatile metals.

4. Nuclear structure of the heaviest elements

Some principle strains of nuclear structure theory are i) the single-particle shell model [18] and the Nilsson model [19], ii) self-consistent mean field approaches [20], iii) the collective model pioneered by Bohr and Mottelson [21], and iv) the interacting boson approximation, IBA. In the following, I will remind the reader of the hybrid model of V.M. Strutinsky in which the binding energy of a nucleus is composed of the liquid-drop model binding energy plus a shell and pairing correction

$$E = E_{\mathrm{LDM}} + \sum_{n,p} (\delta U + \delta P) \tag{5}$$

with the shell correction being

$$\delta U = U - \tilde{U}, \tag{6}$$

with

$$U = \sum_{\nu} 2\varepsilon_{\nu} n_{\nu} \tag{7}$$

being the sum of all single-particle energies in a realistic single-particle model, and

$$\tilde{U} = 2\int_{-\infty}^{\lambda} \varepsilon\, \tilde{g}\,(\varepsilon)\, \mathrm{d}\varepsilon \tag{8}$$

where $\tilde{g}(\varepsilon)$ is a uniform distribution of single-particle states, λ is the chemical potential defined by

$$N = 2\int_{-\infty}^{\lambda} \tilde{g}\,(\varepsilon)\, \mathrm{d}\varepsilon \tag{9}$$

and $N =$ total number of particles. The brilliant philosophy behind this approach is that the systematic errors arising from the calculation of the total energy from a single-particle model will cancel, and only effects associated with the special degeneracies and splitting of levels in the shell-model potential will remain as a shell correction. Looking at, *e.g.*, neutron shell corrections as a function of deformation at and below the $N = 126$ shell, one notices that for spherical nuclei, the correction is negative (corresponding to a larger binding energy) for nuclei at or near closed shells. For mid-shell nuclei, the correction is positive. At $\beta \approx 0.3$ the situation is typically reversed, with a positive correction for nucleon numbers close to the shell closure and a negative one for mid-shell nuclei. This accounts for the observed deformations of these nuclei in their ground states. The shell correction is here large enough to override the favoring of the spherical shape by the liquid drop model part of the total binding energy.

Examples of the nuclear deformation energy for heavy nuclei obtained from Eq. (5) are shown in Fig. 4. The first minimum of the deformation energy occurs at the known deformation of the nuclear ground state. Of special interest is the second minimum in the deformation energy. There is evidence for the presence of such a second minimum in several nuclei from the known existence of spontaneously fissioning isomers, extending from U up to Bk. The second minimum begins to disappear for Cf and heavier nuclei because the liquid drop energy falls off steeply at a smaller deformation as illustrated in Fig. 4. The origin of the second minimum can be visualised when the single-particle energies in the mean potential of all other nucleons are plotted against the deformation of the nucleus expressed in the form of the ratio of the semi-major axis to the semi-minor axis of a prolate ellipsoid. For spherical nuclear shapes, the calculated single-particle energies are well-known to be concentrated periodically in dense groups and the resulting zones of low single-particle density correspond to the known magic nucleon numbers. Periodic fluctuations in the single-particle level density do not only occur as a function of nucleon number but also for fixed nucleon number as a function of deformation. In particular, for nuclear shapes of high symmetry as given by an integer ratio of the half axes of deformed nuclei, again zones of reduced level density occur particularly significantly for a ratio of 2 : 1. The magic numbers associated with these deformations are different from those for spherical nuclei. According to this reason, a Pu nucleus with neutron number 140 should have an enhanced stability against fission compared to its

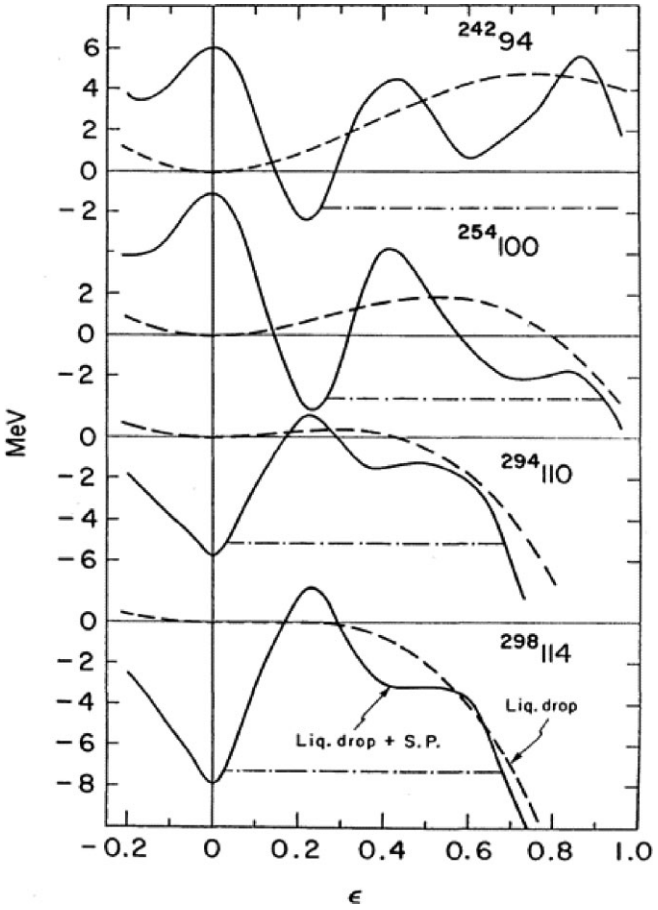

Fig. 4. Potential energy as a function of deformation ε for various heavy nuclei illustrating the effect of shell structure on a liquid drop background. Liquid-drop fission barriers are indicated by the dashed lines. Barriers after inclusion of shell and pairing effects are shown by the solid lines. (Reproduced fromTsang and Nilsson (1970)). Copyright Elsevier Science Publishers B.V. (North-Holland Physics Publishing Division) 1970).

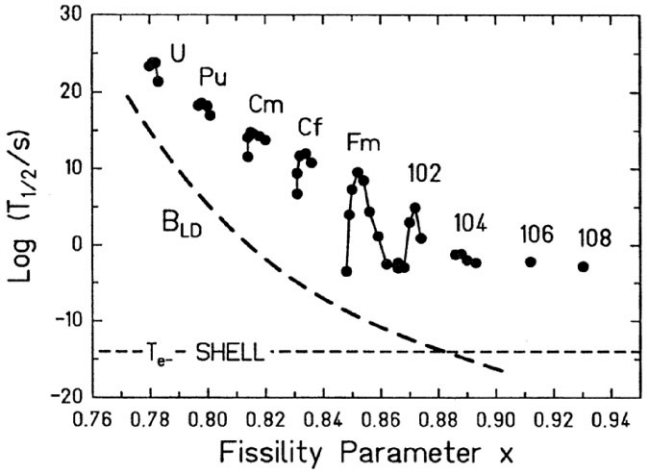

Fig. 5. Systematics of SF half-lives as a function of the fissility parameter x. Experimental data are compared to the prediction of SF half-lives if the fission barriers were those predicted by the liquid-drop model, B_{LD}, and to the time T_{e^-}-SHELL needed to form an electron shell around the nucleus. From G. Münzenberg, S. Hofmann, Discovery of the heaviest elements, in: W. Greiner, R.K. Gupta (eds.), Heavy Elements and related new phenomena. Copyright World Scientific, Singapore, 1999.

Table 1. Comparison of measured and calculated quadrupole moments and ratios of the semi-major to the semi-minor axes in the first and second minimum of ^{239}Pu. From [26].

	1. Minimum	2. Minimum
Q_{exp}	(11.3 ± 0.5) b	(36 ± 4) b
Q_{theor}		38 b Brack *et al.*
(^{240}Pu)		35 b Nerlo-P.
$(c/a)_{exp}$	(1.30 ± 0.05)	(2.0 ± 0.1)

neighbouring nuclei as long as it exhibits a ratio of half axes of 2 : 1.

The lowest excited states of such a superdeformed nucleus correspond to the collective rotation about an axis perpendicular to the symmetry axis. Their energies are determined by the moment of inertia that is increasing with increasing deformation. By the observation of the rotational band in the second minimum of ^{240}Pu, Specht *et al.* [25] obtained a first qualitative hint for the fact that the nuclei in the fission isomeric state are more deformed than the ground state. The moment of inertia was more than a factor of 2 larger than that of the ground state. The moment of inertia, however, is only a strongly model dependent function of deformation, depending on the number of nucleons that participate in the collective rotation of the nucleus. If it would be possible to determine the lifetimes of the rotational states, it would be possible, with the help of the well established rotational model by Bohr and Mottelson, to determine uniquely the quadrupole moment of the nucleus in the fission isomeric state. Due to experimental reasons, D. Habs and V. Metag [26] selected the neighbouring ^{239}Pu for their measurement of the lifetimes of rotational states in the second minimum by the so-called charge plunger technique. Their results are indicated in Table 1 giving a comparison of experimental and theoretical quadrupole moments and deformations in the first and second minimum of ^{239}Pu.

The quadrupole moment in the second minimum is in excellent agreement with theoretical predictions and establishes a ratio of the semi-major axis to the semi-minor axis c/a of exactly 2 : 1. With that, the quantitative proof was delivered that the fission isomers are indeed superdeformed nuclear states that are associated with the existence of a second minimum in the potential energy of deformed actinide nuclei due to shell effects.

As was already evident from Fig. 4, the fission barriers of the heaviest elements are increased by shell effects as compared to the liquid drop fission barriers. Fig. 5 depicts the experimental SF half-lives of the heaviest elements as a function of the fissility parameter x in comparison to the half-lives expected for the liquid drop barriers B_{LD}. For the latter, the lifetime for elements with $Z \geq 104$ would be shorter than the time needed for establishing an electron shell around the nucleus, T_{e^-} SHELL. Thus, according to the liquid drop model, elements with $Z \geq 104$ should not exist. Fig. 5 tells us that, *e.g.*, the most stable isotopes of Rf live roughly 15 orders of magnitude longer than predicted by the liquid drop model. Thus, it is obvious that the superheavy elements are unique in the Periodic Table as they owe their existence solely to nuclear shell effects.

5. Shell stabilization of superheavy elements

There are two ways to look at the details of the stability of superheavy nuclei with respect to the shell closures that are exclusively responsible for their existence. Firstly, one can consider **integral data** for the few atoms that have been synthesized such as SF half-lives, decay modes, and Q_α values. We do this in Fig. 6 depicting SF half-lives as a function of neutron number which also indicates the theoretical predictions of shell closures at $N = 152$ (deformed), $N = 162$ (deformed), and $N = 184$ (spherical). The shell closures at $N = 152$, 162 are well established by experimental data. The theoretically predicted shell closure at $N = 184$, and in particular at $Z = 114$ is lacking experimental verification.

Modern theoretical approaches disagree on the size and position of this proton shell gap. The macroscopic-microscopic models with various parametrizations of the nuclear potential predict $Z = 114$ and $N = 184$. Calculations using self-consistent mean-field approaches broadly fall into two categories, relativistic and non-relativistic ones. In both cases, the splitting between the $2f_{7/2}$–$2f_{5/2}$ spin-orbit partners is not sufficient to open a gap, see Fig. 7. Most non-relativistic mean-field calculations favour $Z = 124$, 126, and $N = 184$, while the relativistic mean-field models show that the effects of magic numbers of a single nucleon configuration that we know from the Sn and Pb shell closures, are dissolved in favour of more extended regions of additional shell stabilization, centred around $Z = 120$, $N = 172$, 184 or $Z = 126$, $N = 184$.

A second way to search for the location of the next spherical shell closure are **spectroscopic studies** in nuclei approaching the "island of stability", such as ^{254}No. Nuclei in this region are deformed, and the degenerate spherical single-particle orbitals split in a well defined way into Nilsson components according to the projection of the angular momentum onto the symmetry axis of the nucleus, the K quantum number. Orbitals originating from above the relevant spherical proton shell such as the $2f_{5/2}$ orbital come close to the Fermi level in a deformed nucleus such as ^{254}No and play a key role in the formation of K isomeric states. In even-even nuclei, the ground state always has $K = 0$. Excited states with large values of K require a decay path back to the ground state that changes this quantum number gradually. If the intermediate K states do not exist, the high K state becomes isomeric. Isomeric states can readily be identified from their decay times and thus give a very clear experimental signature.

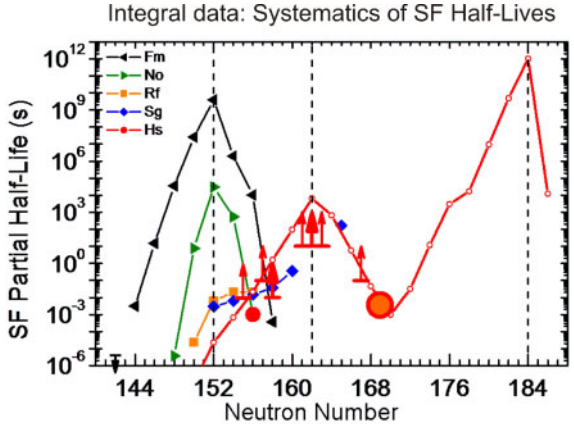

Fig. 6. Spontaneous fission half-lives as a function of neutron number. Experimental data are available for Fm through Hs. Open circles are calculated values by Smolanczuk *et al.* [27] using a macroscopic-microscopic approach.

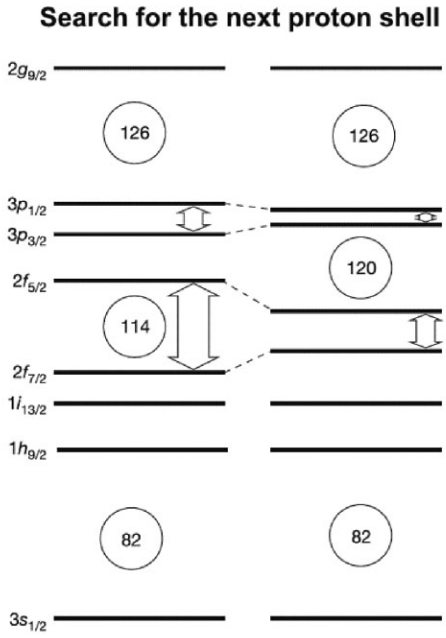

Fig. 7. Illustration of the single-proton energies in superheavy nuclei. The strength of the spin-orbit interaction determines the size of the gap between the $2f_{7/2}$ and the $2f_{5/2}$orbits. To the left is shown the situation in case of a large spin-orbit coupling; to the right, reduced spin-orbit coupling. The spherical levels are labelled with the radial quantum number n, the orbital angular momentum l, and the total angular momentum j, in the standard notation nl_j. The circled numbers are the resulting energy gaps. (Reprinted by permission from Mcmillan Publishers Ltd.: (NATURE) (Herzberg *et al.* (2006), copyright (2012)).

In the work by Herzberg *et al.* [27], ^{254}No was chosen to search for such K isomeric states. It is produced with a reasonable cross section of 2 μb in the ^{208}Pb(^{48}Ca,2n) reaction at 219 MeV. It was separated from unwanted reaction products in the gas-filled separator RITU at Jyväskylä, and was implanted into a double-sided position sensitive Si detector (DSSD) at the center of the GREAT spectrometer. Isomeric states then decayed to the ground state, emitting γ-rays, X-rays, conversion and Auger electrons. These electrons were detected in the same pixel of the DSSD. γ-rays and X-rays were detected in prompt coincidence with this electron signal in a large segmented array of Ge detectors. Finally, the ground state of ^{254}No decays by an 8.1 MeV α decay with a half-life of 51.2 s and is recorded in the same pixel of the DSSD. The decay scheme derived from these studies is shown in Fig. 8. Of relevance for the discussion here is the 3^+ isomeric state. The experimental g-factor identifies the $K = 3$ band head as the two-proton structure $(1/2^-[521]_\pi x 7/2^-[514]_\pi)^{3+}$ involving the $1/2^-[521]$ orbital stemming from the spherical $2f_{5/2}$ orbital above the $Z = 114$ shell. The other stems from the $1h_{9/2}$ proton orbital. This two-quasi-particle proton state, then, can be used by theoretical models as a stepping stone to adjust their parametrizations used in the prediction of the spherical superheavy nu-

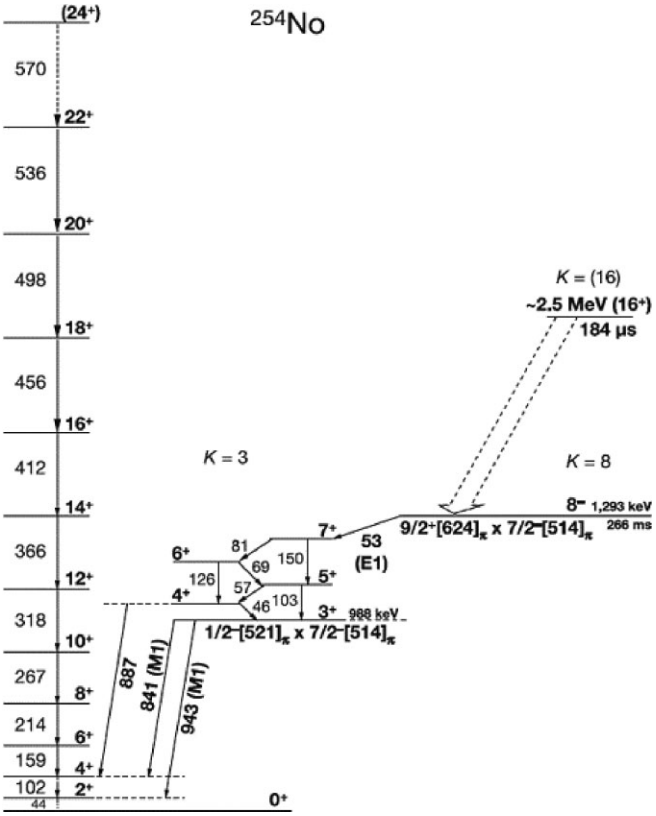

Fig. 8. Level scheme of ^{254}No. The 266 ms 8^- isomer is connected to the ground state *via* an excited 3^+ two-quasi-particle $(1/2^-[521]_\pi \times 7/2^-[514]_\pi)$ band. The 184 µs (16^+) isomer populates the 8^- isomer. Levels are grouped according to the projection of the total angular momentum K on the symmetry axis of the nucleus. (Reprinted by permission from Mcmillan Publishers Ltd.: (NATURE) (Herzberg *et al.* (2006), copyright (2012)).

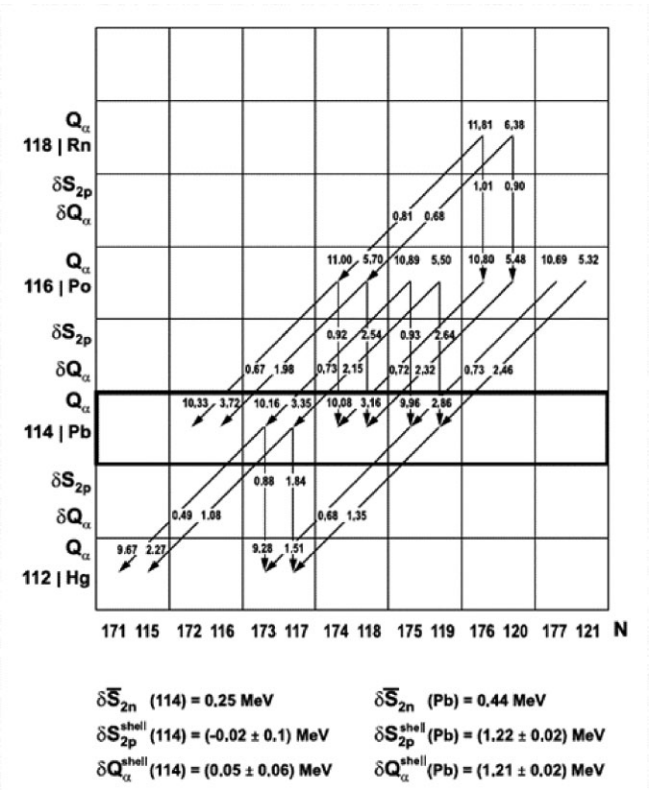

Fig. 9. Measured Q_α values in the 4 decay chains of even elements 112–118 centred at $^{288}_{174}$114 are compared to known Q_α values of elements Rn, Po, Pb, and Hg centred at $^{200}_{118}$Pb. The jump in the values of Q_α and S_{2p} (2-proton separation energy) crossing the shell at $Z = 82$ is analyzed and compared to the corresponding jump at $Z = 114$. While there is a clear jump at $Z = 82$, the analysis shows a smooth transition between the Z values and no indication of a closed shell at $Z = 114$. (Reproduced from Armbruster [28], © Springer-Verlag (2008), with kind permission of the European Physics Journal (EPJ)).

clei, *i.e.* any calculation that gets the 3^+ energy right, also has the $2\,f_{5/2}$ orbital in the right place. At this time, this seems to be a challenge for the self-consistent models where the high l orbitals are systematically shifted to too high energies, *i.e.* the $i_{13/2}$ state ends up between the $f_{7/2}$ and $f_{5/2}$ states removing 114 as a gap.

Returning once more to the **integral data**, I like to discuss work by P. Armbruster [28] who made use of the α-decay energies to search for hints for a shell closure in the FLNR, Dubna, decay chains [29] going through $Z = 114$. These recent experiments demonstrated surprisingly that cross sections for the production of superheavy elements in ^{48}Ca-induced reactions with actinide targets increase beyond $Z = 111$, reach a plateau at a level of 5–10 pb at $Z = 114$ and fall below the 1 pb level at $Z = 118$. α-decay energies for even-even nuclei give access to Q_α values between the ground states of the isotopes involved. The respective chains [29] cross the proposed proton shell at $Z = 114$ at 10 to 12 neutrons below $N = 184$. As the distances between closed shells are 44 neutrons between $N = 82$ and $N = 126$, but 58 neutrons between $N = 126$ and $N = 184$, this difference taken into account reduces the point of comparison to $N = 118$ for the Pb shell. Thus, Armbruster [28] selected chains passing the Pb shell at $N = 119$–116 by the chains descending from Po *via* Pb to Hg and obtained a jump $\delta Q_\alpha^{\text{shell}}(\text{Pb}) = 1.21 \pm 0.02$ MeV. The analysis presented in Fig. 9 demonstrates that the $Z = 82$ shell is still clearly visible at ^{200}Pb and a shell closure at $Z = 114$ should be manifested at $N = 172$ and 174. The analysis shown in Fig. 9 gives $\delta Q_\alpha^{\text{shell}}(114) = 0.05 \pm 0.06$ MeV. Within the uncertainties, there is no shell gap observed at $Z = 114$. A shell closure would be seen not only in the differences of the Q_α values, but also in the 2-proton separation energies S_{2p}. The result of this analysis is similar. While there is a clear jump in $\delta S_{2p}^{\text{shell}}(\text{Pb})$, see Fig. 9, the potential energy surface is smooth showing no closed-shell structure at $Z = 114$ which accompanied superheavy element research since 1966. The next proton shell is filled at $Z > 114$.

The interacting boson approximation, IBA, uses bosons and their symmetries as an ordering principle. The bosons are made of pairs of protons and neutrons, and the symmetries follow from group theory. The model embodies the following assumptions:

- The low-lying excitations of even-even nuclei depend only on the valence space.
- The valence nucleons are treated in pairs, as s and d bosons, with angular momenta 0 and 2. The number of bosons is half the number of valence protons and neutrons, both of which are counted to the nearest proton and neutron closed shells.
- The states of this boson system result from the distribution of the fermions in the s and d pairs, and thus depend

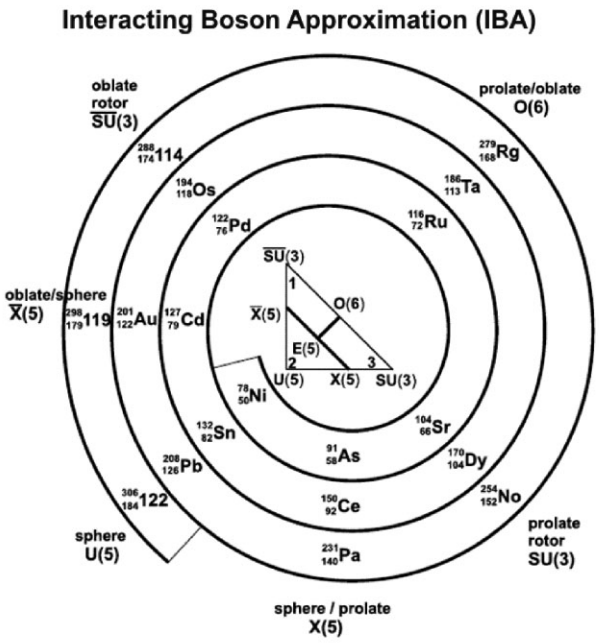

Fig. 10. Interacting boson approximation:The triangle in the center of the figure summarizes the relation between the phase transition points $X(5)$, $O(6)$, and $\overline{X}(5)$ and the shapes $U(5)$, $SU(3)$, and $\overline{SU}(3)$ [22]. The periodicity of nuclear structure is presented by a 3-fold spiral. An extrapolation of the prolate-oblate-spherical phase transitions up to the next doubly magic nucleus $^{306}_{184}122$ is proposed by Armbruster [28], © Springer-Verlag (2008), with kind permission of the European Physical Journal (EPJ).

only on the *s* and *d* boson energies and interactions between them. These interactions are assumed to be simple, at most two-body.

A fundamental feature of IBA is its group theoretical structure. Since an *s* boson has only one magnetic substate and a *d* boson has five, the $s-d$ boson system can be looked at mathematically as a six dimensional space described by the algebraic group structure U(6). This parent group has various subgroups that lead to different dynamical symmetries. There are three of these symmetries that are physically most relevant, known by the labels U(5), SU(3), and O(6). The basic entities of the IBA are the *s* and *d* bosons which are assigned energies ε_s and ε_d. A given nucleus with N_p and N_n valence protons and neutrons each counted to the nearest closed shell has $N=(N_p+N_n)/2s$ and *d* bosons. For example, ^{152}Sm has $N=6+4=10$ and both ^{144}Ba and ^{196}Pt have $N=3+3=6$. No distinction is made whether the valence nucleons are particles or holes. Ground and excited states are formed by distributing the bosons in different ways among *s* and *d* states and coupling them to different *I*. The level structures that result depend on these distributions and couplings. The formalism is phrased in terms of creation and destruction operators for the *s* and *d* bosons. The U(5) symmetry is the IBA version of a spherical vibrator. The SU(3) symmetry is that of the prolate rotor. The O(6) symmetry is corresponding to a deformed, axially symmetric rotor which is γ soft. These are transition nuclei between the prolate rotor (SU(3)) and the oblate rotor ($\overline{SU}(3)$). The symmetry triangle of the IBA is shown in the center of Fig. 10. The three corners are $\overline{SU}(3)\rightarrow 1$, U(5) $\rightarrow$ 2, and SU(3) $\rightarrow$ 3. The transitions between them are involving the symmetry groups X(5) for spherical/prolate, O(6) for prolate/oblate, and $\bar{X}(4)$ for oblate/spherical. The symmetry triangle of the IBA suggests a periodicity of the nuclear structure that is graphically indicated by the threefold spiral in Fig. 10. The latter assigns ^{78}Ni, ^{132}Sn, ^{208}Pb, and ^{306}122 to the spherical U(5) symmetry, ^{104}Sr, ^{170}Dy, and ^{254}No to the SU(3) symmetry, and ^{122}Pd, ^{194}Os, and ^{288}114 to the $\overline{SU}(3)$ symmetry. Prototypes of the transitional nuclei between spherical and prolate are ^{91}As, ^{150}Ce, and ^{231}Pa. Prototypes for the transitional nuclei between prolate and oblate are the triaxially deformed ^{116}Ru, ^{186}Ta, and ^{279}Rg. Prototypes for the transition between oblate and spherical nuclei are ^{127}Cd, ^{201}Au, and ^{298}119. Note that the IBA periodic system would place the next spherical proton shell closure well above $Z=114$ at $Z=122$ in agreement with relativistic mean-field calculations.

According to this ordering principle, the nucleus to be expected as cornerstone in the superheavy element region is $^{306}_{184}122$. The region of spherical nuclei in analogy to the ^{208}Pb region should be expected at $Z=122\pm3$. By traversing the $\bar{X}(5)$ symmetry point at $Z=119$ downwards, a region of oblate shaped nuclei in analogy to the Os region below ^{208}Pb should be entered. It might cover nuclides of the elements 115 ± 3 in the neutron number range $N=174\pm4$ centred around ^{289}115. Thus, all the isotopes discovered recently at the FLNR, Dubna, would have ($\beta_2<0$) deformed oblate shapes. For these potentially oblate isotopes, fission was observed in the isotopes ^{286}114 and $^{282-284}$112. To pass from an oblate shape over a prolate saddle point towards fission may be dynamically hindered. Thus the new superheavy nuclei may have lower fission probabilities. These are the ingredients that Armbruster [28] used to model the production rates for these superheavy nuclei:

The cross section is calculated with a four-factor formula. The factors follow the sequence of stages during the evolution of the fusion reaction:

$$\sigma(Z)=\sigma_{\text{capture}}\cdot p^{\text{hindrance}}(Z)\cdot p^{\text{shape}}\cdot W^{\text{survival}}(Z) \tag{10}$$

The probability $W(Z)$ to survive fission depends on the partial decay widths Γ_n and Γ_f to de-excite by neutron emission (survival) or by fission (destruction), on the excitation energy of the compound nucleus E^* and the number of de-excitation steps until the ground state of the evaporation residue is reached:

$$W^{\text{survival}}(Z)=\prod_{i=1}^{\nu}\left(\frac{\Gamma_n}{\Gamma_n+\Gamma_f}\right)_{(i,E^*)}\approx\left(\frac{1}{1+\Gamma_f/\Gamma_n}\right)^{\nu} \tag{11}$$

The ratio Γ_n/Γ_f, given an excitation energy E^* and temperature T, depends on the ratio of level densities above the neutron separation energy B_n and the fission barrier B_f:

$$\Gamma_n/\Gamma_f=K\frac{\exp\left(E^*-B_n\right)/T}{\exp\left(E^*-B_f\right)/T}=K\exp\left[-\left(B_n-B_f\right)/T\right] \tag{12}$$

with $K=1.4A^{2/3}T$, and A the mass number of the compound system. This holds for "actinide based" 4*n* and 5*n* reactions, *i.e.* for $E^*>B_n>B_f>T$. For 50 MeV excitation energy, the value of $\Gamma_n/(\Gamma_n+\Gamma_f)$ is close to 0.4. For small excitation energies, the value becomes smaller; for 12 MeV,

the value sinks to 10^{-2}. The latter is a question of time scales. The time for fission is typically 3×10^{-20} s; the time for neutron emission at 12 MeV excitation energy is 10^{-17} s.

According to the macroscopic-microscopic model, the fission barrier $B_f = B_{LDM} + \delta U$, and Γ_n/Γ_f thus depends on the shell correction energy:

$$\Gamma_n/\Gamma_f = K \exp\left[-\left(B_n - B_{LDM}\right)/T\right] \cdot \exp\left(\delta U/T\right) \qquad (13)$$

For superheavy elements, B_{LDM} is smaller than the zero-point vibrational energy and can completely be ignored. According to A.V. Ignatyuk, δU is damped by excitation energy:

$$\delta U = \delta U_0 \exp\left(-\gamma E^*\right) \quad \text{with}$$
$$\gamma^{-1} = 5.48A^{1/3}/\left(1 + 1.3A^{-1/3}\right) \qquad (14)$$

For deformed evaporation residues, the $1/e$ damping energy is 27 MeV for hot fusion reactions. For spherical heavy nuclei, this is different: For Th isotopes from 1*n* to 4*n* reactions close to the spherical neutron shell $N = 126$, as models for spherical superheavy elements, the work by Vermeulen *et al.* [30] shows that for the 4*n* reactions, there is no gain in cross sections due to the shell closure. Only for the lowest excitation energies (Zr isotopes on ^{124}Sn), *i.e.* for the 1*n* channel, there is an indication for a small gain in cross sections at $N = 126$. The mechanism that reduces Γ_n/Γ_f for spherical nuclei has been called "collective enhancement of level densities" and has been introduced by T. Ericson in 1958; it was further worked out by S. Bjørnholm and B. Mottelson in 1974. The enhancement factor K_{coll} of the level densities is different for ground-state level densities, that determine Γ_n, and for saddle-point level densitites that determine Γ_f. At the saddle point, the finite deformation of the nucleus causes a high level density due to rotational excitations which is not the case for the spherical ground state.

The two factors $\sigma_{capture}$ and $W(Z)$ allowed for a presentation of fusion induced by α particles and light ions on actinide targets. Elements up to $Z = 106$ were synthesized and correctly described. Cross sections down to 10 nb were reached. The excitation energy of the compound system in nearly symmetric collision systems is $E^* \approx 0$, and for $B_f > B_n$ seemed possible without fission losses, that is by capture alone at $W(Z) \to 1$. First estimates in 1967 by T. Sikkeland to produce superheavy elements gave cross sections of 100 mb. These were the times when the elements Rf and Db were discovered, and synthesis of superheavy elements became a major goal of nuclear chemistry.

In the first SHIP experiments, the production of superheavy elements at the closed neutron shell $N = 184$ was envisaged. The nearly symmetric reaction $^{136}\mathrm{Xe} + {}^{170}\mathrm{Er} \to {}^{306}_{184}122^*$ and $^{65}\mathrm{Cu} + {}^{238}\mathrm{U} \to {}^{303}_{182}121^*$ were investigated in 1976/1977 by P. Armbruster *et al.* Instead of cross sections in the 100 mb range, a limit below 1 nb was established. The discrepancy between expectation and the observed result by 8 orders of magnitude showed that fusion is governed by more physical processes than capture and de-excitation. New processes, *i.e.* deep-inelastic collisions and quasi-fission, were discovered to take the missing flux toward fusion. Recent calculations by W. Swiatecki *et al.* [31] confirm the exponential decrease of the reaction flux. P. Armbruster used the formula

$$p^{hindrance}(Z) = C \cdot \exp\left[-\left(0.5/\log e\right)\left(Z - Z_0\right)\right] \qquad (15)$$

and assumed that Eq. (13) is valid for all mass asymmetries of the collision system. Hindrance sets in at a certain threshold Z_0 which is smallest for symmetric fusion.

The factor p^{shape} in Eq. (9) takes into account the dependence of the fission probabilities on the shape of the nuclei to be produced. Nearly everything that is known about fission concerns nuclei with prolate deformations in the ground state and these pass over a prolate saddle point towards scission. For these nuclei, p^{shape} is set equal to one. For oblate nuclei, there is a possible stabilisation against fission discussed above. This is taken care of by a common gain factor $p^{shape} = 10$ for all the oblate isotopes of the elements concerned. For spherical nuclei, on the other hand, collective enhancement of level densities at the saddle point, as discussed above, reduces the survival of the compound system. The spherical nuclei neighbouring the spherical shell $N = 126$ for the elements 87–91 were found to show fission probabilities increased by a factor of 100 compared to their deformed neighbours. In the range of superheavy elements, $Z = 119$–126 close to the spherical neutron shell $N = 184$, the same behaviour is expected. At least the same loss factor 10^{-2} should be introduced in p^{shape} for the spherical superheavy nuclei.

The Ignatyuk formula, Eq. (14), is used in the form $K_D = \exp(-\gamma E^*)$ where K_D may take values between no damping, $K_D = 1$, and the Ignatyuk value. Armbruster fixed the value at $K_D = 0.7$ by adjusting the calculated cross sections to the FLNR values. Thus staying within well-known physics, Armbruster was able to reproduce the FLNR cross sections as is shown in Fig. 11. The increase in the range

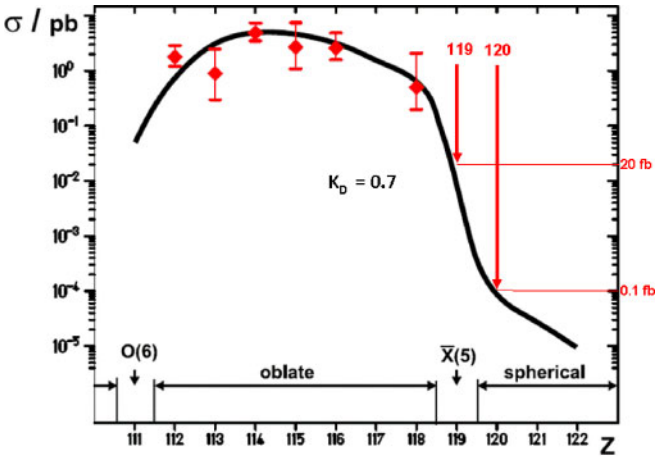

Fig. 11. Cross sections for production of superheavy elements demonstrating both the increase beyond $Z = 111$ and the decrease beyond $Z = 118$ reaching a value of 10^{-5} pb at $Z = 122$ according to P. Armbruster [28]. Besides the steady decrease by the hindrance factor $p^{hindrance}$, the transition from oblate to spherical nuclides between $Z = 118$ and $Z = 120$ introduced by the shape factor p^{shape} is demonstrated. Whether the breakdown beyond $Z = 118$ by three orders of magnitude is realistic remains to be seen. However, even without this breakdown, $\sigma(Z)$ would reach for $Z = 122$ a limit of 10 fb which is not accessible with today's experimental techniques. (Adapted from Armbruster [28], © Springer-Verlag (2008), with kind permission of the European Physics Journal (EPJ)).

$Z = 111$ to $Z = 115$ is connected with the gain factor for all the oblate isotopes in this range but also with the fact that the foot of the ascent to the doubly closed-shell nucleus $^{306}_{184}122$ at the top has been traversed. With $B_f > B_n$, $Z = 118$ is reached with a survival close to one. The factor p^{shape} has been set to 10^{-2} for the spherical nuclides above $Z = 118$ which is causing the precipitous decrease of the cross sections beyond. Collective enhancement of level densities destroys these nuclei as has been shown for their $N = 126$ partners. This figure suggests that it will be very challenging to try to go beyond $Z = 118$.

6. Conclusions

The impact of the heaviest elements on the Periodic Table of the elements is that, at this time, nearly one quarter of all elements are man-made transuranium elements that do not exist in nature. They have altered the architecture of the Periodic Table by introducing an actinide and a superactinide series.

The impact of the heaviest elements on chemical science is that their chemical properties are strongly influenced by relativistic effects. These change the properties in a given group of the Periodic Table in a non-linear fashion. There are primary and secondary relativistic effects and the strong spin-orbit splitting. Relativistic sub-shell closures have given rise to a new category of elements in the Periodic Table: These are volatile metals.

In the physical science, the remarkable role of the transuranium elements is that nuclear shell effects dominate their structure and stability. These shell effects give rise to superdeformed shape isomers (fission isomers) in the actinides (U–Bk). Superheavy elements ($Z \geq 104$) are unique elements that owe their stability exclusively to nuclear shell effects centred at $N = 152$, $N = 162$, and $N = 184$. At this time, a building lot is the question for the location of the next spherical proton shell. This urgently needs further theoretical and experimental efforts. The cross sections for the syntheses of $Z = 119$ and $Z = 120$ will give us important information about the "upper end of the Periodic Table of the elements".

Acknowledgment. The author is indebted to the Bundesministerium für Bildung und Forschung BMBF for financial support under contract 06MZ223I and to the Helmholtz Intitute Mainz HIM for the reimbursement of travel expenses. Thanks are due to N. Wiehl for help with the figures.

References

1. Mendeleev, D.: Z. Chem. **12**, 405 (1869).
2. Meyer, L.: Liebigs Ann. Chem. Suppl. **7**, 354 (1870).
3. Mendeleev, D.: Liebigs Ann. Chem. Suppl. **8**, 133 (1871)
4. Seaborg, G. T.: The chemical and radioactive properties of the heavy elements. Chem. Eng. News **23**, 2190 (1945).
5. Seaborg, G. T.: Evolution of the modern periodic table. J. Chem. Soc., Dalton Trans. 3899 (1996).
6. Fricke, B., Greiner, W., Waber, J. T.: The continuation of the periodic table up to $Z = 172$. The chemistry of superheavy elements. Theor. Chim. Acta **21**, 235 (1971).
7. Fricke, B., Waber, J. T.: Model calculations on the influence of electrodynamical effects on the chemistry of superheavy elements. The chemistry of E184. Act. Rev. **1**, 433 ((1971).
8. Baerends, E. J., Schwarz, W. H. E., Schwerdtfeger, P., Snijders, J. G.: Relativistic atomic orbital contractions and expansions: magnitudes and explanations. J. Phys. B **23**, 3225 (1990).
9. Desclaux, J. P.: Relativistic Dirac–Fock expectation values for atoms with $Z = 1$ to $Z = 120$. At. Data Nucl. Data Tab. **12**, 311 (1973).
10. Pershina, V., Fricke, B.: Relativistic effects in physics and chemistry of element 105. IV. Their influence on the electronic structure and related properties. J. Chem. Phys. **99**, 9720 (1993).
11. Pitzer, K. S.: Are elements 112, 114 and 118 relatively inert gases? J. Chem. Phys. **63**, 1032 (1975).
12. Pershina, V.: Relativistic electronic structure studies on the heaviest elements. Radiochim. Acta **99**, 459 (2011).
13. Pershina, V., Anton, J., Jacob, T.: Theoretical predictions of adsorption behaviour of elements 112 and 114 and their homologues Hg and Pb. J. Chem. Phys. **131**, 084713 (2009).
14. Eichler, R., Aksenov, N. V., Belozerov, A. V., Bozhikov, G. A., Chepigin, V. I. *et al.*: Chemical characterization of element 112. Nature **447**, 72 (2007).
15. Eichler, R., Aksenov, N. V., Belozerov, A. V., Bozhikov, G. A., Chepigin, V. I. *et al.*: Thermochemical and physical properties of element 112. Angew. Chem. Int. Ed. **47**, 3262 (2008).
16. Eichler, R., Aksenov, N. V., Albin, Yu. V., Belozerov, A. V., Bozhikov, G. A. *et al.*: Indication for a volatile element 114. Radiochim. Acta **98**, 133 (2010).
17. Yakushev, A., Gates, J. M., Türler, A., Schädel, M., Düllmann, Ch. E. *et al.*: Superheavy element 114 is a volatile metal. Nature (London), submitted (2012).
18. Mayer, M. G., Jensen, J. H. D.: *Elementary theory of nuclear shell structure*. Wiley, New York (1955).
19. Nilsson, S. G.: Binding states of individual nucleons in strongly deformed nuclei. Dan. Mat.-Fys. Medd. **29**, 16 (1955).
20. Bender, M., Heenen, P.-H., Reinhard, P.-G.: Self-consistent mean-field models for nuclear structure. Rev. Mod. Phys. **75**, 121 (2003).
21. Bohr, A., Mottelson, B. R.: Collective and individual particle aspects of nuclear structure. Dan. Mat.-Fys. Medd. **27**, 16 (1953); Collective Nuclear Motion and the Unified Model. (Siegbahn, K., ed.) North Holland, Amsterdam (1955).
22. Arima, A., Iachello, F.: Collective nuclear states as representations of a SU(6) group. Phys. Rev. Lett. **35**, 1069 (1975); Interacting boson model of collective states I, The vibrational limit, Ann. Phys. **99**, 253 (1976); Iachello, F.: *Interacting Bosons in Nuclear Physics*. Plenum, New York, (1979).
23. Strutinsky, V. M.: Shell effects in masses and deformations. Nucl. Phys. A **95**, 420 (1967).
24. Tsang, C. F., Nilsson, S. G.: Shape isomeric states in heavy nuclei. Nucl. Phys. A **140**, 275 (1970).
25. Specht, H. J., Weber, J., Konecny, E., Heunemann, D.: Identification of a rotational band in the ^{240}Pu fission isomer. Phys. Lett. B **41**, 43 (1972).
26. Habs, D., Metag, V.: Messung extremer Kerndeformation von Spaltisomeren. Phys. Bl. **34**, 647 (1978).
27. Herzberg, R.-D., Greenlees, P. T., Butler, P. A., Jones, G. D., Venhart, M. *et al.*: Nuclear isomers in superheavy elements as stepping stones towards the island of stability. Nature Lett. **442**, 896 (2006).
28. Armbruster, P.: Shifting the closed proton shell to $Z = 122$ – a possible scenario to understand the production of superheavy elements $Z = 112$–118. Eur. Phys. J. A **37**, 159 (2008).
29. Oganessian, Yu.: Heaviest nuclei from ^{48}Ca-induced reactions. J. Phys. G: Nucl. Part. Phys. **34**, R165 (2007).
30. Vermeulen, D., Clerc, H.-G., Sahm, C-C., Schmidt, K.-H., Keller, J. G., Münzenberg, G., Reisdorf, W.: Cross sections for evaporation residue production near the $N = 126$ shell closure. Z. Phys. A **318**, 157 (1984).
31. Swiatecki, W., Siwek-Wilczynska, K., Wilczynski, J.: Fusion by diffusion. II. Synthesis of transfermium elements in cold fusion reactions. Phys. Rev. C **71**, 014602 (2005).